Martin Lévesque,[1] Michael D. Gilchrist,[2] and Bohuslav Fisa[3]

A Theoretical Study of the Tensile Test for Highly Anisotropic Composite Materials

---

Reference: Lévesque, M., Gilchrist, M. D., and Fisa, B., **"A Theoretical Study of the Tensile Test for Highly Anisotropic Composite Materials,"** *Composite Materials: Testing and Design Fourteenth Volume, ASTM STP 1436,* pp. 320-335, C. E. Bakis, Ed., ASTM International, West Conshohocken, PA, 2003.

Abstract: The stress field in a tabbed straight-sided tensile test specimen has been studied theoretically and experimentally. It is shown that the stress field has to be studied at every point in the specimen. It is also shown that the tab should be made as thick as possible and the clamping force set as large as possible in order to minimize the intensity of the stress field in the specimen. The tab's Young's modulus in the test direction is the elastic constant having the largest influence on the stress field in the specimen. However, it is shown that it is not possible to set general guidelines regarding the choice of the tabs material. Failure modes of specimens where the tabs are bonded and where the tabs are molded directly on the test material were compared. Molded specimens produce better quality results.

Keywords: tensile test, anisotropy, tab, composite materials, failure, strength

Introduction

One of the most fundamental mechanical properties for a unidirectional (UD) material is its ultimate strength in the fiber direction. Due to the nature of UD materials and to the fact that it is very difficult to create a purely axial stress field in a tensile specimen, some difficulties can be encountered when attempting to measure this property.

Various standard procedures (ISO, ASTM, etc.) exist for measuring the tensile strength of composite laminates. However, situations can arise when, even if they are followed with great care, these standards fail to produce acceptable results [*1*]. In such cases, the standards do not provide the experimentalist with guidelines to modify the specimen in order to improve the quality of results. The aim of this paper is to present a detailed analysis of the stress field in a tensile test specimen in order to give guidelines for improving the quality of results when measuring the tensile strength in the fibre direction of a UD composite material. A brief literature review is followed by finite element simulations of the tensile test. General recommendations are given and results obtained from a case when ASTM Test Method for Tensile Properties of Polymer Matrix Composites Materials (D 3039) – referred as ASTM D 3039 in the remaining of the paper – fails to produce acceptable failures are compared with those obtained by following the recommendations of this present study.

---

[1] ENSAM Paris - Laboratoire LM3, 151 Boul. de l'Hôpital, 75013 – Paris, France.
[2] Senior Lecturer, NUI Dublin, Dept. of Mech. Engineering, Belfield, Dublin 4, Ireland.
[3] Professeur, Ecole Polytechnique Montréal, Département de Génie Mécanique, C.P 6079 Succ. Centre-ville, Montréal (Québec), Canada, H3C 3A7.

Background

Conventions and Definitions

This paper is concerned solely with composites that are made of prepregs with long unidirectional fibers. The standard axes convention is used where the 1-2-3 subscripts refer to material directions and the x-y-z subscripts refer to loading directions. Unless otherwise specified x and 1 directions coincide. The capital letters "X", "Y" and "Z" refer to the strengths in the 1, 2 and 3 directions while "S" refers to the shear strength. The subscripts "t" and "c" refer to tension and compression (i.e. X_t is the tension strength in the 1 direction). Superscript "t" refers to the tabs material (i.e. E_{11}^t is the E_{11} modulus of the tab). The "test material" defines that volume occupied by material being tested (i.e., gauge section + transition + clamping zone). The "parasitic stresses" are defined as all components of stress other than σ_{11}. The "gauge section" identifies the volume in which the stress field is assumed to be constant and purely axial (i.e. no parasitic stresses) and from which failure initiates/occurs.

Specimen Shape

Various geometries, including the "bow tie" or "stream line" [*2, 3*] specimen and the ASTM Test Method for Tensile Properties of Plastics (D 638) "dog bone" specimen, have been recommended. However, failure of UD materials loaded in the fiber direction, usually initiates where the cross-section changes. In addition, the bow tie and stream line specimens require careful and expensive manufacturing. For these reasons, the general specimen shape considered by this study is a rectangular flat strip, as recommended by ASTM D 3039. From a deterministic perspective, this geometry is also flawed since a concentration of the axial stress and parasitic stresses arises due to the load introduction (clamping). Failure of this geometry would, in principle, initiate in a complex stress field and thus lead to the material tensile strength being underestimated. However, for hand layup laminates and in order to reduce the coupon preparation costs, this geometry seems to be a reasonable compromise.

In order to protect the gauge section from the clamping effects, some authors [*4,5*] suggest using flat strip specimens with a $[90/0_4]_S$ layup. With an appropriate approach, the strength of the 0° plies can be calculated. The experimental results show that the strength measured with this specimen is higher than with a conventional flat strip. However, a micromechanical analysis is required to show that the reinforcing plies do not change the natural failure mode of the material. The results obtained from such specimens must be interpreted with care and for this reason, such a specimen is not considered in the present study.

Square Tabs vs. Tapered Tabs

Experience has shown that bonded tabs are required when measuring X_t [*6*]. However, there is no agreement regarding tab shape [*7*]. For example, Hojo et al. [*7*]

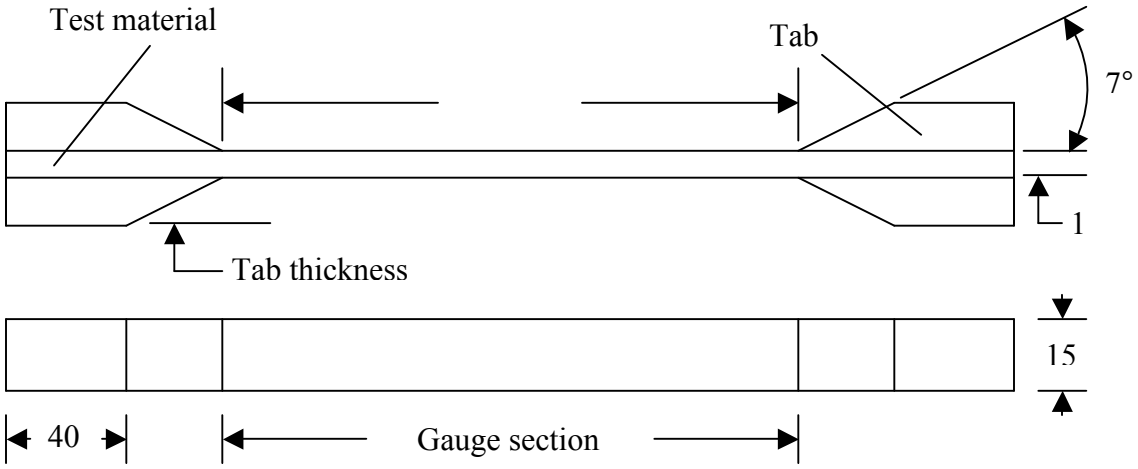

Figure 1 – *General Specimen Shape*

have shown experimentally that there is no statistical difference in X_t when tapered or square glass/epoxy tabs are bonded to carbon epoxy materials. It should be noted, though, that the authors observed some debonding problems with the tapered tabs and it is difficult to determine if this is due to inadequate tab bonding or to the tab shape itself. Other work [*8,9*], however, has shown that bonded tapered tabs reduce the scatter and increase the average value of X_t. Wisnom et al. [*10*] and Green and Shikhmanter [*11*] tested specimens where tapered tabs are moulded directly to the specimen. When an appropriate layup sequence was used to manufacture the tab, the mean value and scatter of X_t were also improved [*10*]. This avoided the bonding problems between tab and test material. However, these authors [*8-11*] did not conduct a sufficient quantity of replicas to statistically prove the effect of the taper.

Some authors [*5, 9, 12-14*] have theoretically shown that the concentration of σ_{11} and the intensity of σ_{22}, σ_{33} and σ_{13} in the gauge section decrease when the taper angle decreases. Kural and Flaggs [*12*], however, have shown that σ_{33} is lower for a straight tab when the tab is fully clamped on its top surface. Nevertheless, it is the other parasitic stresses that are more important for the straight tab than for a low taper angled tab. Cunningham et al. [*9*] have shown that a feather edged tapered tab generates lower intensity parasitic stresses than a tab with a drop-off.

Based on these theoretical observations and on the fact that experiments have not conclusively shown that one configuration is better than another, this study will concentrate on feather edged tapered tabs. Since the effect of the taper angle has been studied, it will be fixed to a value of 7° (for manufacturing simplicity) for this study, as suggested by ASTM D 3039. Figure 1 shows the general specimen shape studied here.

Stress Field in the Tension Specimen

Figures 2 and 3 show a typical distribution of σ_{11}, σ_{22}, σ_{33} and σ_{13} in the test material near the tab / specimen interface. The parasitic stresses are seen to exhibit two local maxima, identified as points A and B. In Figure 3, point B is where all the

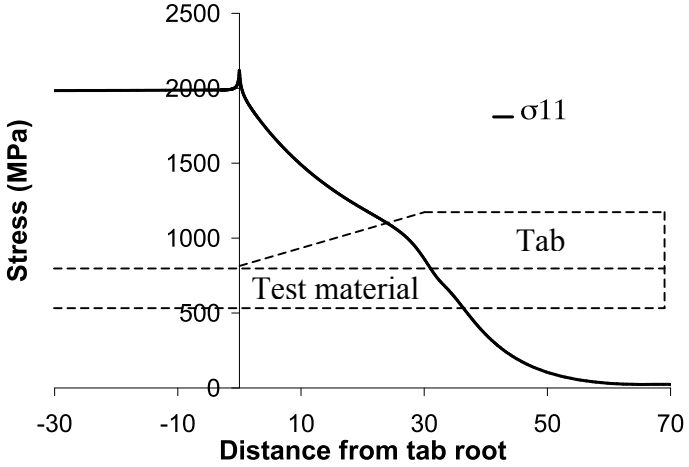

Figure 2 – *Axial Stress in the Test Material*

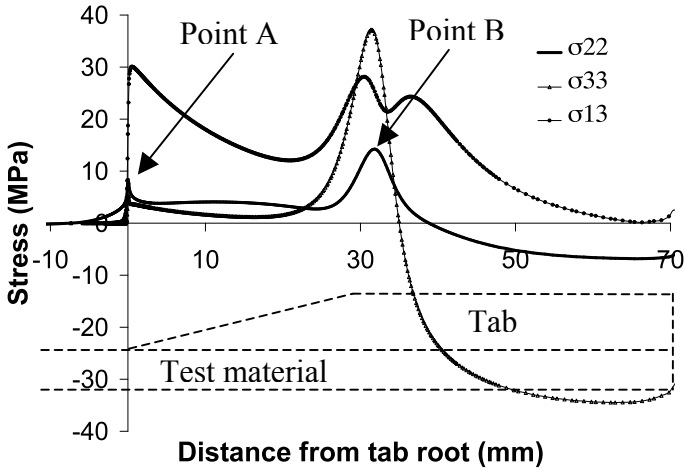

Figure 3 – *Parasitic Stresses in the Test Material*

parasitic stresses peak, while Kural and Flaggs [*12*] obtained a maximum at point A for all these stresses (for a different specimen material – tab material configuration). This indicates that the taper's root is not the only point where the stresses have to be estimated but the whole stress field has to be taken into account. It should be noted that no author has previously addressed the interaction effect of the parasitic stresses.

Cunningham et al. [*9*] and Kural and Flaggs [*12*] have shown that the tab thickness and length have a negligible influence on the generation of parasitic stress at point A for a tapered tab (point B was not discussed). Some authors have studied the influence of the tab material on the parasitic stresses including steel and aluminium [*5,14*], glass/epoxy [*4 ,9, 12, 14*] and carbon/epoxy and polyamide 66 [*14*]. All these authors showed that the intensity of the parasitic stresses at point A decreased when E^t_{11} decreased. It should be noted that the influence of the other elastic constants were not discussed.

Some authors have computationally analysed the influence of the adhesive between the tab and the test material [*5, 9, 15*]. There is no agreement on the influence of thickness and ductility of the adhesive on the parasitic stresses. It would seem that

these divergences are associated with the particular finite element meshes used since the element refinement and numerical integration schemes were different for each author. Since experimental difficulties were encountered with bonded tabs [*1*], it was decided to manufacture specimens where the tab is molded to the specimen. Consequently, this study is not concerned with the influence of the adhesive.

Discussion

Even though the tensile test has been closely studied, some issues remain outstanding:

1. The influence of the geometric and material parameters of the tab on the stress field should be estimated at all points (not only at point A).
2. The influence of tab elastic constants (in the case of an anisotropic material) on the stress field in the specimen should be discussed. This would provide guidelines for the choice of tab material.
3. The parasitic stresses have previously been studied separately. It would be interesting to estimate, with a failure criterion, the influence of the interaction of all these stresses in order to identify potential failure initiation points.

It has not yet been mentioned, but the influence of the clamping force on the parasitic stresses has not been studied theoretically. This study addresses these four issues.

Finite Element Simulations of the Tensile Test

Model Description

The geometry has already been described in Figure 1. For practical reasons, the gauge section has been fixed to 250 mm, the gripping length on the tab to 40 mm and the taper angle to 7°. The tab is made of a woven glass/epoxy composite while the test material is a UD carbon/epoxy. Table 1 lists the properties (supplied by manufacturer) that were used in the FE model (unless otherwise specified).

The FE calculations were conducted using ABAQUS 5.8. 20-noded second order brick elements (8500 per model) were used since stress concentrations were to be estimated and the elements near the root of the taper were distorted by the small taper angle. The loading and boundary conditions are illustrated in Figure 4. For symmetry reasons, only one quarter of the specimen was modelled. It is assumed that no slip occurs between the grips and the specimen and that the grip and tab remain

Table 1 – *Base Materials Mechanical Properties*

	E_{11} (GPa)	E_{22} (GPa)	E_{33}* (GPa)	ν_{12}	ν_{13}*	ν_{23}*	G_{12} (GPa)	G_{13}* (GPa)	G_{23}* (GPa)
Glass/epoxy	17	17	15	0.24	0.4	0.4	5	5	5
Carbon/epoxy	126	11	11	0.28	0.4	0.4	6.6	6.6	6.6
	X_t (MPa)	X_c (MPa)	Y_t (MPa)	Y_c (MPa)	Z_t* (MPa)	Z_c* (MPa)	S_{12} (MPa)	S_{13}* (MPa)	S_{23}* (MPa)
Glass/epoxy	360	240	360	205	40	100	98	98	98
Carbon/epoxy	1950	1480	48	200	48	200	79	79	79

*Assumed values

fully in contact during the whole test. The mesh was refined in areas of high stress gradients until a convergent solution was obtained in these areas.

For each model, the x displacement was imposed iteratively until σ_{11}=1950 MPa in the gauge section. A friction coefficient of 1 was assumed between the grip and the tab. The z displacement was iteratively modified until the sum of the reaction forces at the nodes in the z direction equated the reaction force in the x direction in the gauge section. The stresses and strains were extracted at the elements integration points.

Stress Field in the Specimen

Figures 2 and 3 have shown the stress field as a function of the specimen length for tabs of 3 mm thickness. For all models, the stresses are calculated in the test material at 0.011 mm under the specimen's surface and 0.14 mm from the mid-width since all stress components peaks along this line.

It can be seen from Figure 2 that σ_{11} increases by approximately 6.5% at point A. Using a weakest link theory with a Weibull distribution (see [*16*] for an example), assuming that there are no parasitic stresses and integrating the σ_{11} stress field over the whole volume shows that this stress concentration has a negligible effect on the value of X_t measured by the tensile test (see [*1*] for a more detailed discussion).

As shown on Figure 3, other parasitic stresses are present (σ_{12} and σ_{23} were not plotted, as they were negligible in comparison to the other stresses). Unlike σ_{11}, it is not possible to use a weakest link theory to model the failure in the other directions [*16*]. In addition, at this time, no macroscopic failure criterion provides an accurate failure prediction [*17*]. For these reasons, and for simplicity, the interaction between the parasitic stresses is taken into account by a polynomial failure criterion of form:

$$f = F_i\sigma_i + F_{ij}\sigma_i\sigma_j \qquad \textbf{(1)}$$

where *f* is the failure index and F_i and F_{ij} are constants that are a function of the ultimate strengths. Failure occurs if *f* reaches a value greater than 1.0. After some simplifications and by neglecting $F_{i=j}$, the failure criterion takes the form:

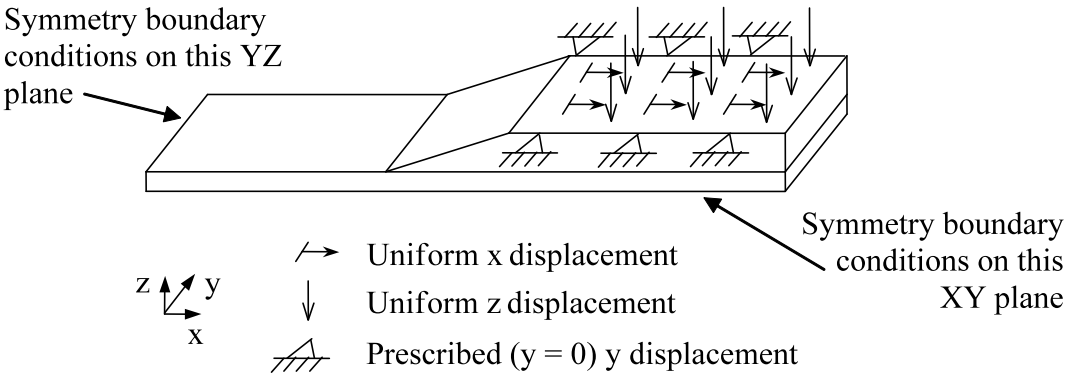

Figure 4 – *Boundary Conditions*

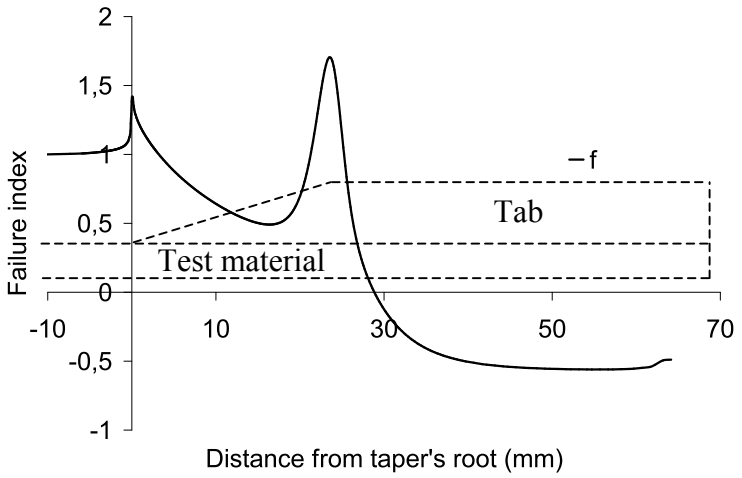

Figure 5 – *Failure Index in the Test Material*

$$f = \left(\frac{1}{X_t} + \frac{1}{X_c}\right)\sigma_{11} + \left(\frac{1}{Y_t} + \frac{1}{Y_c}\right)\sigma_{22} + \left(\frac{1}{Z_t} + \frac{1}{Z_c}\right)\sigma_{33} - \frac{\sigma_{11}^2}{X_t X_c} - \frac{\sigma_{22}^2}{Y_c Y_t} - \frac{\sigma_{33}^2}{Z_t Z_c} + \frac{\sigma_{13}^2}{S_{13}^2} \qquad \textbf{(2)}$$

This failure criterion is used to compare different test configurations. It is also used to compare the sensitivity to failure initiation at various points in the specimen. For example, for the base case (tab 3 mm thick), Figure 5 shows the evolution of the failure index 0.011 mm below the surface of the specimen and 0.14 mm from the mid-width as a function of the x axis. It can be seen that the failure index peaks at point B, showing that failure is likely to initiate under the tab.

It should be noted that the parasitic stresses do not show stress concentrations along the specimen's width and thickness [*1*]. All the parasitic stresses have a relatively constant magnitude along the specimen's thickness and width, except for σ_{22} which varies from zero (on the specimen side) to a certain value (at the mid-width of the specimen) across the specimen's width. For these reasons and for the fact that all parasitic stresses peak at 0.011 mm under the specimen's surface and 0.14 mm from the mid-width, it was decided to not present their evolution in this paper (the whole 3D stress field can be found in more in details in [*1*]).

Influence of Tab Elastic Constants on the Stress Field in the Specimen

In order to estimate the effect of a variation of the engineering constants of the tab on the stress field in the specimen, a statistically designed experiment was used. A full two modalities factorial design was used. The modalities were chosen so that the upper modality was 30% higher than the lower modality for all the elastic constants. The engineering constants varied were E_{11}^t, E_{22}^t, G_{13}^t and ν_{12}^t. The other elastic constants were not studied in order to limit the number of FE models built. For the 16 models, the boundary conditions were adjusted iteratively until σ_{11} = 1950 MPa in the gauge section. The peak stresses and failure index at point A and B were extracted at the integration points. The analysis of variance was conducted by considering the

Table 2 – *Linear Regression Coef f icients*

		Response variable				
Point	Constant	σ_{11}	σ_{22}	σ_{33}	σ_{13}	f
A	E_{11}	16,1196*	1,006*	0,7432	4,2046*	0,0713*
	E_{22}	0,2131	0,0256	0,0059	0,0104	0,0010
	G_{13}	1,9997*	0,0291	-0,0022	0,0443*	0,0033
	ν_{12}	1,2795*	-1,7005*	0,0428	0,2376*	-0,0263*
B	E_{11}		-1,0340*	-3,8581*	-2,6713*	-0,1432*
	E_{22}		-0,5564*	-0,4805*	-0,067577	-0,0189*
	G_{13}		0,9829*	1,5509*	1,2060*	0,0632*
	ν_{12}		-1,9708*	0,1545*	0,2964*	-0,0360*

*Statistically significant

variability associated with the second order interactions as the experimental variability. For each of the components of stress and for the failure index, a linear regression was performed having the form:

$$\hat{\sigma}_{ij} = \rho E_{11}^t + \chi E_{22}^t + \lambda G_{13}^t + \psi \upsilon_{12}^t + \overline{\sigma}_{ij} \quad \textbf{(3)}$$

where the Greek letters are the coefficient of the linear regression and $\overline{\sigma}_{ij}$ is the average stress. Table 2 reports the value of these regression coefficients. It should be noted that σ_{11} is not given at point B since point B is defined as the point where the parasitic stresses peak and it that it was shown that σ_{11} only peaks at point A in figure 2. The average value was not included since it depends on the geometrical parameters not included in the model. Since all dependant variables were changed by the same relative value, the numerical value of each regression coefficient can be interpreted as the sensitivity of a given stress to that elastic constant. Under these conditions, the numerical values of the regression coefficients can be compared to each other to establish if one elastic constant is more influential than another. In addition, the sign of the coefficient indicates if the intensity of a parasitic stress increases or decreases when a given elastic constant increases. For all the dependent variables, the minimum value of the modified R^2 coefficient is 98%, which shows that the first level interaction regression model explains the variability reasonably well. Second and higher order interactions can thus be neglected.

It can be seen from Table 2 that E_{11}^t is the engineering constant having the largest effect on the failure index at points A and B. In addition, it can be seen that the sum of the effect of all the other constants is lower than the effect of E_{11}^t (for both points). Point B seems to be more sensitive than point A to E_{11}^t. However, it can be observed that the effect of E_{11}^t is opposite at points A and B. It is impossible, therefore, to give a general recommendation as to the numerical value that E_{11}^t should take in order to simultaneously reduce the value of the failure index at points A and B. The same reasoning can be applied to the other engineering constants. Unlike E_{11}^t, general

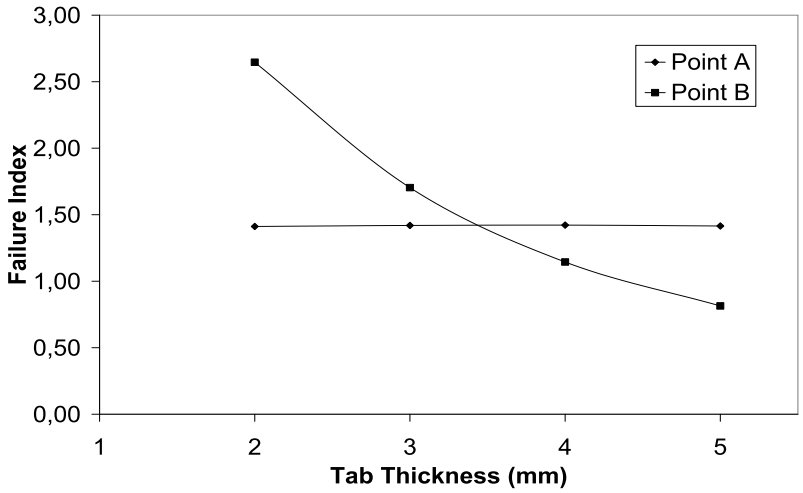

Figure 6 – *Peak Failure Index as a Function of Tab Thickness at Points A and B*

recommendations can be given for the other elastic constants. The tab material should be chosen to ensure that E_{22}^{t} and ν_{12}^{t} are as high as possible while G_{13}^{t} should be as low as possible.

It should be noted that these results are valid for materials similar to UD carbon/epoxy composites. The failure index depends on the failure strengths in the various directions of the material. In addition, the stress field is affected by the ratio of the elastic constants of the tab and test material. For a different material, the sensitivity of the failure index to the engineering constants could be more or less important. A formal continuum mechanics analysis is required to address these issues.

Influence of the Tab Thickness on the Stress Field

The tab thickness was modified from the base model while all the other dimensions were kept constant. The thickness was varied from 1mm to 5mm (a higher value might not be practical since it could be impossible to clamp into the traction machine).

Figure 6 shows the evolution of the failure index at points A and B as a function of the tab thickness. For the simulated case, it can be observed that point A is relatively insensitive to the tab thickness while point B is greatly affected by the tab thickness. In addition, the peak point of the failure index shifts from point B to point A as the thickness increases. It could be generally recommended to use the thickest tab possible. It should be noted that increasing the tab thickness, while maintaining all the other geometrical parameters constant, increases the bond line length between the tab and the test material. In this area, the mean value of σ_{13} decreases since the area where the traction force is applied increases. This would partially explain why the failure index at point B decreases with the tab thickness.

Influence of the Clamping Force on the Stress Field

Table 3 - *Influence of the Clamping Force on the Parasitic Stresses and on f*

	Pressure (MPa)	σ_{11}	σ_{22}	σ_{11}	σ_{33}	f
Point A	-34,69	2078	8,25	5,07	29,48	1,42
	-41,61	2077	8,25	5,06	29,47	1,41
	-55,05	2076	8,24	5,06	29,45	1,41
	-69,07	2074	8,23	5,05	29,42	1,41
	-139,32	2070	8,21	5,04	29,36	1,40
	-209,70	2061	8,17	5,02	29,24	1,39
Point B	-34,69		9,39	29,02	25,54	0,81
	-41,61		9,06	26,73	25,53	0,76
	-55,05		8,61	23,33	25,50	0,68
	-69,07		8,31	20,69	25,48	0,62
	-139,32		8,19	14,48	21,02	0,50
	-209,70		8,97	12,73	23,47	0,85*

*The peak failure index occurs at a different point

The base model was simulated with 5 mm thick tabs and 6 different clamping forces. Table 3 lists the minimum σ_{33} and the parasitic stresses, as well as the failure index at points A and B. It can be seen that the failure index at point A is slightly affected by the clamping force while it is affected more at point B. Globally, σ_{33} decreases at point B when the clamping force is increased. However, if the clamping force is too important, the failure index increases at a different point on the specimen as Z_c is almost reached. Therefore, the clamping force should be as high as possible without causing compressive failure of the specimen.

Discussion

In order to reduce the peak failure indices in the tensile specimen studied in this paper, the following guidelines are applied:

- The tab material should be chosen so that G_{13}^t is as low as possible while E_{22}^t and ν_{12}^t are as large as possible. It is not possible to give such a general guideline for the numerical value of E_{11}^t. Tabs made of an appropriate layup sequence of a composite material would appear to be a better choice than using an isotropic material such as aluminium or steel.
- The thickness of the tab should be as large as possible to reduce the parasitic stresses under the tab.
- The clamping force should be as high as possible while avoiding the premature failure of the specimen.

In light of these observations and with the choice of materials that were available for experiments, the following specimen configuration was chosen:

Tabs: Made of a woven-glass epoxy prepreg, oriented at ± 45°. This layup sequence is symmetrically balanced to reduce the shear coupling and the interlaminar peeling stresses. The tab geometry is the same as the base model but the thickness is

Table 4 – *SuggestedSpecimen vs ASTM D3039 Specimen*

	σ_{11}	σ_{22}	σ_{33}	σ_{13}	f	
Point A	2047	1,75	8,75	25,02	1,24	Suggested specimen
Point B		-0,04	23,50	25,54	0,52	
Point A	2078	7,61	5,14	29,54	1,41	ASTM D 3039
Point B		35,05	64,43	58,82	2,65	

4.5 mm. This was the maximum thickness enabling a proper insertion of the specimen into the traction machine.

Clamping force: The z displacement was iteratively modified until the maximum value of σ_{33} was 60% of the estimated compressive strength of the specimen. The reaction forces at the nodes were calculated and this resulting force was identified as the clamping force.

This configuration was simulated and the peak failure indices at points A and B were calculated. The specimen configuration recommended by ASTM D 3039 was simulated using the same tab material. The results are compared in Table 4. It can be seen that the failure indices at points A and B were simultaneously reduced using the configuration suggested by this study. However, for the current configuration, the failure index at point A is still above 1.0. Since the geometry cannot be changed significantly, the tab material could be chosen so that this failure index decreases. For example, a layup sequence where the apparent E_{11}^t would be smaller than the one simulated could decrease the failure index at point A while increasing the failure index at point B. The material should be chosen so that the failure index at point B does not exceed 1.0.

Experimental analysis

Prior to this study, an attempt was made to measure the tensile strength of a UD carbon epoxy material by following ASTM D 3039. Some modifications to the adhesive and the tab material were made in order to achieve acceptable results, but without success. It was then decided to undertake the theoretical study presented in Section 3 to guide the choice of the specimen configuration. This section presents the experimental results obtained in the preliminary study. These results are then compared with those obtained with the specimen designed in this study.

In order to compare the 'quality' of the results, a design allowable $R_{0.95}$ has been calculated for each set of experiments. This value is the stress at which 95% of all the samples of a given population failed. Since a relatively small number of runs were carried out for each test, the population was assumed to be normal. In addition, the standard deviation γ and the average μ were estimated by a 95% confidence interval. With the appropriate combination of the upper and lower bounds of these estimates a 95% confidence interval for $R_{0.95}$ was calculated. If the confidence interval for $R_{0.95}$ for the two experiments are not overlapping it will be concluded that an experiment has given better quality results than the other.

Experimental Setup

Table 5 – *Tab Material and Adhesives Used in the Preliminary Study*

Tab	
Type 1	± 45° Woven glass/epoxy composite. E_{11}^t = 25 GPa. Tab 3.2 mm thick
Type 2	± 45° Woven glass/polyester composite. E_{11}^t = 5.3 GPa. Tab 2 mm thick
Adhesive	
Type 1	High resistance cyanoacrylate instantaneous adhesive. Manufactured by Loctite under the trade mark Super Attack Gel
Type 2	High performance ductile epoxy adhesive. Manufactured by 3M under the trade mark DP – 460

All the tests were carried out on an Instron 8500 tensile machine with a 50 kN load cell. Strain gauges were bonded to the specimens to estimate any misalignment of the jaws, as detailed in the ASTM D3039 standard. In addition, strain gauges were bonded to measure torsion in the specimen. For all experiments, the torsion and bending were within acceptable limits.

The samples were clamped to the desired value in the hydraulic grips. Since every specimen failed catastrophically, X_t was calculated by dividing the maximum recorded load by the initial cross section A of the gauge section.

Preliminary Study

Specimen Preparation

The aim of this preliminary study was to establish the influence of various tab-adhesive configurations on the measured X_t. The tab materials and adhesives used are listed in Table 5. The test material was cut with a diamond saw from flat panels. The panels were moulded from 5 plies (0.26 mm thick) of UD carbon/epoxy prepregs having a 60% fibre volume fraction. The test material was supplied by epo-faser-technik GmbH (Germany) under the product name PR FB 1361 205/1000 FT102 48%. The mechanical properties given by the supplier are listed in Table 1. Five each of four different specimen combinations (Tab1-Adhesive1, etc.) were manufactured. The tabs were carefully bonded to the specimens by following manufacturers' recommendations for optimal bond strength.

Experimental Results

Most of the specimens failed by transverse splitting. No debonding was observed for the specimens made with adhesive 1, while some problems were encountered with adhesive 2. Some failures clearly initiated at point B (see [*1*] for more details).

Due to the small number of replicas and the considerable scatter, it was impossible to show statistically that one combination was better than another. All the results were combined and the Shapiro-Wilk test for normality failed to show that the population was not normal. By assuming that the population is normal, a confidence interval for $R_{0.95}$ was calculated. The numerical results are reported in Table 6.

It can be seen that $R_{0.95}$ calculated is not very useful and is below the generally

Table 6 – *Comparison of the Experimental Results*

	Parameter	Lower Bound	Estimation	Upper Bound
Preliminary Study	μ (MPa)	1335	1483	1630
	γ (MPa)	222	297	444
	$R_{0.95}$ (MPa)	605	995	1264
Suggested Specimen	μ (MPa)	1668	1820	1972
	γ (MPa)	90	145	355
	$R_{0.95}$ (MPa)	1084	1582	1823

accepted value of 2000 MPa for this kind of material. In addition, the coefficient of variation is around 20%, which is higher than the generally accepted value of 5%.

This is an example of how the ASTM D 3039 specifications can fail to provide acceptable results, even if followed with care and some attempts are made to improve the quality of the results.

Specimen Suggested by this Analysis

Specimen Preparation

The tabs were molded directly on to the test material. In addition, a mold was manufactured so that every specimen was moulded separately. The gauge section was made of 5 plies of the same material described in the preliminary study and the tab layup sequence was $[+45/-45]_{s3}[+45/-45]$ using a woven glass epoxy prepreg manufactured by epo-faser-technik GmbH (Germany) under the product name PR UD C(UTS) ST 170/600 FT102 38% (properties are listed in table 1).

It should be noted that the mould used for these experiments was flawed and some difficulties were encountered when removing the specimens from the mould. Some specimens were broken whilst others were damaged. Only those specimens which had no evident damage were chosen for the tests. Six specimens that were considered "acceptable" were manufactured before failure of the mould.

Experimental Results

No tab debonding was observed. The failure modes varied from transverse splitting, to brush-like, to explosion. It was impossible to identify the point of failure initiation, as it was not possible to remove the tabs to inspect the test material.

Table 6 lists the confidence intervals for the mean, standard deviation and $R_{0.95}$. Here again, the confidence interval of $R_{0.95}$ is quite wide and does not represent a practical interest. This was to be expected due to the small number of observations, since the confidence interval on the standard deviation is quite sensitive to the number of observations.

Discussion

Figure 7 shows that the confidence intervals for $R_{0.95}$ are overlapping. It is

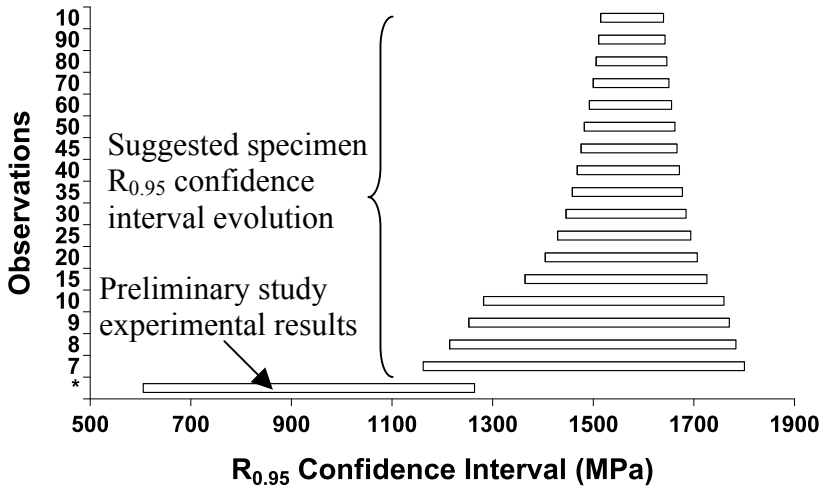

Figure 7 – *Evolution of $R_{0.95}$ Confidence Interval vs Number of Observations*

therefore impossible, with this amount of statistical information, to determine if the quality of the results obtained with one testing configuration is better than the other. However, the estimates of the mean and standard deviation are of better 'quality' for the configuration suggested by this study.

It should be noted that this reasoning is based on few observations. It could be possible that more observations would confirm that the configuration developed by this study gives better quality results. For example, if it is assumed that the standard variation and mean remain relatively constant, Figure 7 shows that for 10 observations (4 more) the two confidence intervals would not overlap. Even though the results are not statistically significant, they are promising.

It should be further noted that the upper bound of $R_{0,95}$ (see table 6) is still below the value given by the manufacturer (1950 MPa). This is probably due to the fact that the manufacturer usually cuts tensile test coupons in the middle of large plates, where the fibres orientation is almost constant. In this study, the specimens were moulded individually and fibre misalignement was present due to resin flow in the mold. Moulding plates where tabs are included and cutting the coupons from these plates (while not including in the analysis the coupons obtained from the side of the plate) could improve the quality of the results.

Conclusion

This theoretical and experimental analysis has shown that:

1. For materials similar to those simulated in this study, increasing the value of E_{22}^t and ν_{12}^t and decreasing the value of G_{13}^t decrease the peak intensities of the parasitic stresses and the failure index in the test material.
2. The most influential tab engineering constant on the parasitic stress field in the test material is E_{11}^t. However, the effect of this elastic constant is opposite at points A and B. The tab material must then be chosen so that the failure index is as low as possible at both points.

It should be noted that this study is a particular case of a wide variety of tab

material – test material combinations. A theoretical continuum mechanics analysis (if possible) or simulating a wider range of material configurations would be necessary to identify a range of tab material suitable for different test materials. Such results would be useful for experimentalists in determining their initial choice of tabbing fixtures.

3. The clamping force should be as high as possible while avoiding compressive failure of the test material.

A theoretical study linking the clamping force applied on the tab to the maximum σ_{33} in the specimen is required to guide the choice of the clamping force. This would help the experimentalist to adjust his traction machine.

4. Manufacturing samples where the tab is directly moulded on the test material can be used successfully to eliminate the bonding problems and to use full advantages of the tapered tab.

There is scope for a more detailed study on the choice of the layup sequence for the tab. In addition, it would be interesting to develop an efficient and economical procedure to mould the whole specimen. This manufacturing technique is promising and could be affordable for composite manufacturers or researchers having access to manufacturing equipment.

References

[1] Lévesque, M. *L'essai de traction de matériaux composites unidirectionnels à fibres continues (Masters Thesis)*. École Polytechnique de Montréal. 2000.

[2] Oplinger, D.W., Gandhi, K. and Parker, B. "Studies of Tension Test Specimens for Composite Material Testing", Technical report, Army Materials and Mechanics Research Center, AMMRC TR 82-87, USA, 1982.

[3] Oplinger, D.W., Parker, B.S., Gandhi, K.R., Lamothe, R. and Foley, G., "On the Streamline Specimen for Tension testing of Composite Materials", *Recent Advances in Composites in the United States and Japan, ASTM STP 864*, 1985, pp. 532-555.

[4] Chatterjee, S., Adams, D. and Oplinger, D.W. "Test Methods for composites: A Status Report, Volume I, Technical Report", DOT/FAA/CT-93/17, I, USA, 1993.

[5] Chatterjee, S., Yen, C.-F. and Oplinger, D.W. "On the determination of Tensile and Compressive Strength of Unidirectional Fibre Composites", *Composite Materials: Fatigue and Fracture (Sixth Volume), ASTM STP 1285*, 1987, pp. 203-224.

[6] Frovel, M., Pintado, J.M., Garcia, J.L. and Arribas. "Collaborative test programme results for 0° tensile properties on carbon-epoxy AS4/8552 and carbon-cyanate M55J/954-3 composite materials and some considerations on EN 2561 test standard", *Plastic, Rubber and Composites*, Vol. 28, No.9, 1998, pp. 425-431.

[7] Hojo, M., Sawada, Y. and Miyairi, H. "Influence of clamping method on tensile

properties of unidirectional CFRP in 0° and 90° directions – round robin activity for international standardization in Japan", *Composites*, Vol. 25, No. 8, 1993, pp. 786-796.

[8] Abdallah, M.G. and Westberg, R.L. "Effect of tab design of the ASTM D3039 Tension Specimen on Delivered Strength for HMS1/3501-6 Graphite/Epoxy Material", *Proceedings, 1987 SEM Spring Conference in Experimental Mechanics*, 1987, pp. 362-366

[9] Cunningham, M.E., Schoultz, S.V. and Toth, J.M. Jr. "Effect of End-Tab Design on Tension Specimens Stress Concentrations", *Recent advances in Composites in the United States and Japan, ASTM STP 864*, 1985, pp. 253-262.

[10] Wisnom, M.R., Jones, M.I. and Cui, W. "Failure of Tapered Composites Under Static and Fatigue Tension Loading", *AIAA Journal*, Vol. 33, No. 5, 1995, pp. 911-918.

[11] Green, A.K., Shikhamanter, L. "Coupon development for fatigue testing of bonded assemblies of pultruded rods", *Composites part A: applied science and manufacturing*, Vol. 30, 1998, pp. 611-613.

[12] Kural, M.H., Flaggs, D.L. "A Finite Element Analysis of Composite Tension Specimens", *Composites Technology Review*, Vol.5, No.1, 1983, pp. 11-17.

[13] Pai, D.M., Kelkar, and Dandy, L.T. "Investigation of In-Grip Failure in Composite Tensile Coupons by Finite Element Analysis", *American Society of Mechanical Engineers (paper) Winter Annual Meeting*, 1993, pp. 1-3.

[14] Tsuji, N., Kubomura, K. "Effect of Poisson's ratio on CFRP tensile test coupon failure", *National SAMPE Technical Conference on Advanced Materials: Looking Ahead to the 21st Century 22nd International SAMPE Technical Conference*, Vol. 22, 1990, pp.1146-1155.

[15] Xie, M. and Adams, D.F. "Tab Adhesive in a Composite Compression Specimen" *Polymer Composites*, Vol. 16, No.6, 1995, pp. 529-535.

[16] Wisnom, M.R. "Size effects in the testing of fibre-composite materials", *Composites Science and Technology*, Vol. 59, 1999, pp.1937-1957.

[17] Soden, P.D., Hinton, M.J. and Kaddour, A.S. "A comparison of the predictive capabilities of current failure theories for composite laminated", *Composites Science and Technology*, Vol. 58, 1998, pp. 1225-1254.